SAJSET
ISSN: 2992-3581

Savannah Journal of Science and Engineering Technology
Volume: 03; Issue: 04; Pages: 260-269; 2025.
www.sajsetjournal.com.ng

DOI: xx.xxxx.x/sajset-03-2025-0035

SAJSET
ISSN: 2992-3581

An optimized artificial neural network based maximum power point tracking for photovoltaic systems using chicken swarm optimization

[1]Aminu, M., [1]Jival, A., [1]Buni, D. and [2]Adamu, A.
[1]*Department of Electrical and Electronics Engineering, Modibbo Adama University, Yola, Nigeria*
[2]*Department of Electrical and Electronics Engineering, Adamawa State Polytechnic, Yola, Nigeria*
jival.angeti@mau.edu.ng, bunidlamatukuli@gmail.com, elabbaszfy@gmail.com,

Paper History
Received: 12th July, 2025
Accepted: 19th August, 2025
Published: August, 2025

Corresponding author
Aminu, M.
aminumhd@mau.edu.ng

Abstract:
Conventional Maximum Power Point Tracking (MPPT) methods suffer from low accuracy and slow response under rapidly changing weather and load conditions. This paper proposes an enhanced training technique to improve the performance of conventional Artificial Neural Network (ANN)-based MPPT for photovoltaic (PV) systems. The method employs the Chicken Swarm Optimization (CSO) algorithm to determine the optimal network topology, weights, and bias values. The proposed ANN-based MPPT model takes solar irradiance and temperature as inputs to predict the voltage corresponding to the Maximum Power Point (MPP). This predicted voltage serves as a reference and is compared with the actual PV voltage to generate an error signal. The resulting error is used to regulate the duty cycle of the PWM signal driving the DC-DC boost converter. Meteorological data collected from the Modibbo Adama University weather station were used to ensure accurate ANN training and real-world applicability. A comprehensive PV system model including solar panels, a DC-DC boost converter, MPPT controllers, and varying loads was developed using MATLAB/Simulink to evaluate the proposed CSO-ANN MPPT method. Simulation results under various operating scenarios show that the proposed CSO-based tuning method gave the best ANN network topology with optimum weights and bias values. This significantly improves its power tracking performance compared to the conventional Perturb and Observe (P&O) method. The proposed approach achieved the lowest ripple factor of 10.01%, in contrast to 32.02% obtained with the conventional P&O algorithm.

Keywords: *Artificial neural network, Maximum power point tracking, Photovoltaic*

1. Introduction

Solar energy remains the fastest growing and most widely used renewable energy resource for electricity generation. This is evident by the steady rise in global Photovoltaic (PV) installed capacity [1]. According to Solar Power Europe [2], it took just about a decade for the global PV installed capacity to reach 1 TW, from 100 GW in 2012. The urgent need for clean energy and the declining costs of PV systems have been identified as crucial factors responsible for this exponential growth. In addition, solar cells and modules are ideal energy generators that have no moving parts and rely on a virtually limitless energy source, namely, the sun [3].

However, despite the numerous benefits of PV systems, one notable disadvantage is the poor performance in terms of efficiency. Only about 18% to 22% of solar energy is being transformed into electricity by the most efficient PV cell [4, 5]. This is because of the non-linear I-V (Current-Voltage) characteristics of the PV cells which are dependent on the irradiation level, temperature of the cell and the load [5]. In order to maximize the amount of energy produced by a PV system, it is important to develop a control mechanism that allows the system to operate at the Maximum Power Point (MPP) despite the inherent changes in solar irradiation levels and temperature. One of such methods is the Maximum Power Point Tracking (MPPT) algorithm. MPPT is a control strategy that enables PV modules to generate maximum power they are capable of producing under all possible environmental and operating conditions by adjusting the electrical operating points of the system.

Although several MPPT methods exist in practice and in literature, the most common method used is the classical Perturb and Observe (P&O) method [6]. However, one main drawback of this method is that it fails under rapid variation in solar irradiance and temperature [6]. This happens when the change in power because of operating conditions is larger than the change produced by the P&O algorithm which may result in shifting the operating point in the opposite direction [6]. The Incremental Conductance (INC) method was proposed for rapidly changing atmospheric conditions but require complex steps and expensive controls [7].

The optimization methods such as Gray Wolf Optimization (GWO) and MayFly (MF) have been used to accurately track maximum power of PV system under complex environmental conditions [8 – 10]. Both methods show great response speed and accuracy in MPPT under partial shading conditions. Nonetheless, their search spaces are large and calculation time is long.

Artificial intelligence based MPPT methods have been proposed to improve the dynamic performance of MPP tracking. Concentrating on nonlinear characteristics of the PV arrays, the artificial intelligence methods such as Fuzzy Logic (FL) and Artificial Neural Network (ANN) provide a fast, yet, computationally demanding solution for the MPPT problem [7]. The advantage of FL is that no need of mathematical model of the PV system when designing a controller. However, the disadvantage is the complexity in selection and tuning of membership functions and designing of fuzzy rules [11]. ANN on the other hand requires no detailed information about the system. Once trained, ANN is capable of tracking complex nonlinear systems. The drawbacks of ANN are the requirement for large training data and as a result, large storage space which makes the technique a bit costly. Also, parameter tuning (weights and bias) may be required for accurate tracking of M [11, 12]. In addition, expert knowledge of the system is required in tuning of parameters [6].

The hybrid MPPT algorithm combines the intelligent algorithm and the classical MPPT method [13 - 15] or the Optimization method and the artificial intelligent method [5, 16]. Such methods combine the advantages of the algorithms, but usually involve complex algorithms and are difficult to implement [17 – 19].

In recent year, new powerful optimization algorithms have been proposed to enhance the performance of ANN MPPT system [16, 20]. In this research an intelligent training method is proposed for improving the conventional ANN-MPPT for PV system using Chicken Swarm Optimization (CSO) algorithm. The CSO-Trained ANN will solve the problem of the choice of ANN topology and parameter tuning during training. Real data from Metrological station and simulation setup in MATLAB/SIMULINK is used for training to ensure accuracy of the ANN when operating in the field.

2. Materials and methods

The basic arrangement of a standalone PV system for powering a DC load comprises the following basic components: PV array, power electronic converter (DC-DC boost converter), MPPT controller and a DC load. The PV array delivers power to a standalone or grid connected system through a DC-DC boost or buck converter. The MPPT system controls the DC-DC converter switching for maximum power extraction. Figure 1 shows the proposed NN-MPPT controller. Solar radiation (G) and temperature (T) data are feed to the NN-MPPT to compute the power reference which is compared to the PV array measured power to obtain an appropriate duty ratio for switching the DC-DC converter. The CSO algorithm helps in training the ANN-MPPT for optimum weights, bias and topology for maximum power tracking [20].

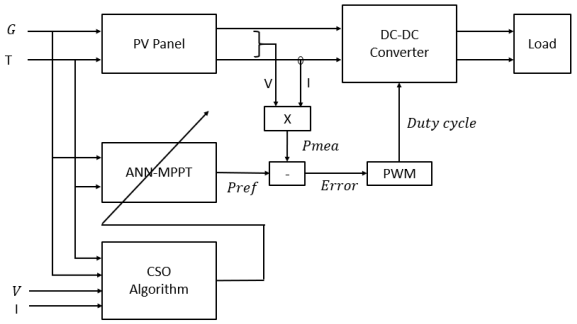

Figure 1: Complete diagram of a standalone PV system with ANN-MPPT controller

2.1 PV system modelling

The mathematical model representation of the different PV system blocks shown in Figure 1 are covered in the following subsections:

2.1.1 PV panel model

The most common electrical equivalent circuit of a solar cell is shown in Figure 2. It comprises a photo-current source (I_{pv}) connected in parallel with a diode D, characterizing the junction of semi-conductors which make the solar cell, and a parallel and series resistance (R_p) and (R_s) respectively [21].

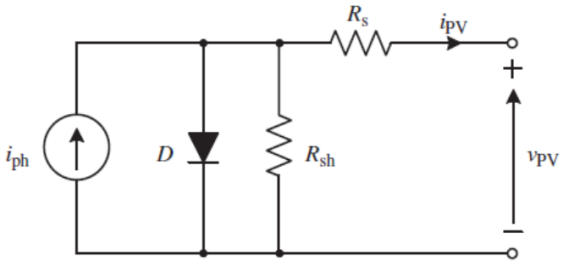

Figure 2: Equivalent circuit of a typical solar cell

The I-V characteristics of a PV cell can be described by equation 1 [6]:

$$i_{pv} = i_L - i_0\left(e^{\left(\frac{v_{pv}+i_{pv}R_S}{\frac{nkT}{q}}\right)} - 1\right) - \frac{v_{pv}+i_{pv}R_S}{R_{sh}} \quad (1)$$

Where: v_{pv}: output voltage of the solar cell, i_{pv}: output current of the solar cell, i_L: photo current, i_0: reverse saturation resistance, T: temperature of the solar cell, R_s: series cell resistance, R_{sh}: shunt cell resistance, n: ideality factor $(1 < n < 2)$, k: Boltzman's constant, q: electron charge.

The current of the PV cell at MPP depends linearly on the solar irradiation and is also influenced by the temperature according to the equation while Voltage at MPP is largely independent of irradiance but decreases with temperature as given in equations 2 and 3 respectively [6]:

$$i_{mpp} = i_{mpp-ref}\left(\frac{G}{G_{ref}}\right)\left(1 + \alpha\left(T - T_{ref}\right)\right) \quad (2)$$

$$v_{mpp} = v_{mpp-ref}\left(\beta\left(T - T_{ref}\right)\right) \quad (3)$$

Where: G is the solar irradiance at current conditions (W/m²), G_{ref} is the reference irradiance (typically 1000 W/m²), T is the module temperature (°C), T_{ref} is the reference temperature (typically 25°C), $i_{mpp-ref}$ is the MPP current at G_{ref} and T_{ref}, $v_{mpp-ref}$ is the MPP voltage at G_{ref} and T_{ref}, α is the temperature coefficient of i_{mpp}, β is the temperature coefficient of v_{mpp}.

2.1.2 DC-DC boost converter

DC-DC boost converters shown in Figure 3 work on regulating and stepping up the input voltage of a solar array to match the load requirement and also serve as an interface for the MPPT algorithm. The DC-DC boost converter performance depends on the input impedance and the connected load R_L which should be selected such that it is greater than the MPP resistance (R_{mpp}). The tracking region for the boost converter can therefore be changed by varying the duty cycle (D), such that the load impedance is matched with the source impedance to attain the maximum power from the PV panel [22]. D is calculated by using equation 4 [23]:

$$D = 1 - \sqrt{\frac{R_{mpp}}{R_L}} \quad (4)$$

The values of the converter components will be obtained based on the PV panel power

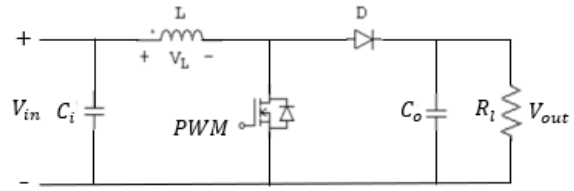

Figure 3: DC-DC boost converter circuits

The inductor two capacitors are crucial and must be carefully calculated. For continuous conduction mode (CCM) of operation, the inductor is obtained by equation 5 [22, 23]:

$$L = \frac{V_{in}D}{\Delta I_L f_s} \quad (5)$$

Where: V_{in} is the input voltage, f_s is the switching frequency and ΔI_L is the inductor current ripple (usually 20%–40% of average inductor current)

Also, average inductor current is given by equation 6:

$$I_L = \frac{I_{out}}{1-D} \quad (6)$$

To maintain a steady output voltage with limited ripple and to reduce input voltage ripple, an output and input capacitors are used and are calculated by equations 7 and 8 respectively: [22]:

$$C_o = \frac{DI_{out}}{\Delta V_{out} f_s} \quad (7)$$

$$C_i \geq \frac{DI_{out}}{\Delta V_{in} f_s} \quad (8)$$

Where: ΔV_{out} and ΔV_{in} are the allowed output and input voltage ripple respectively.

For a boost converter the output voltage is obtained by equation 9 [22]:

$$V_{out} = \frac{V_{in}}{1-D} \quad (9)$$

2.1.3 Design of CSO-tuned ANN-MPPT

A three-layer Feedforward Neural Network (FNN) is used to track the MPPT. As shown in Figure 4, the proposed system has irradiance and temperature as inputs and voltage of MPP as the output. This voltage termed the reference voltage is compared to the measured voltage to obtain an error signal to adjust the duty ratio of the PWM signal to the DC-DC boost converter. For training purpose, it is necessary to obtain large data as inputs and target output. Different number of hidden layers were tested to train the network. In the conventional ANN, the backpropagation algorithm is widely used for updating the weights and bias of the network.

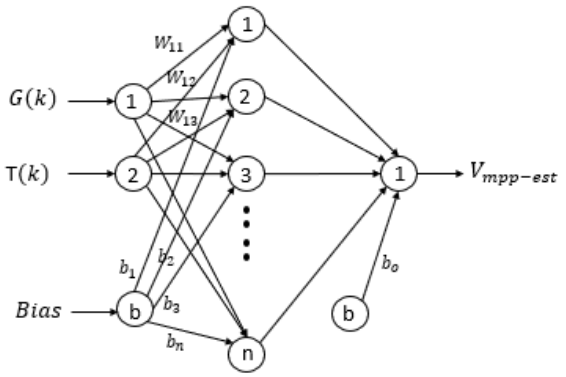

Figure 4: Artificial neural network architecture

Base on Figure 4, the different layers of FNN are given in equations 10 -14 [24]: Input layer 1:

$$u_j^1 = p_j \quad (10)$$

Where $j = 1,2,\ldots n$ (number of inputs)

Hidden layer 2:

$$u_k^2 = \eta(FNN_k^2) \quad (11)$$

$$FNN_k^2 = \sum_j\left(w_{kj}^2 . u_{kj}^{2-1}\right) \quad (12)$$

Output layer 3:

$$q_{predicted} = \eta(FNN^3) \quad (13)$$

$$FNN^3 = \sum_j\left(w_j^3 . u_j^2\right) \quad (14)$$

Where $q_{predicted}$ is the predicted output, w_{kj}^2 is the weight connection between the j^{th} neuron of the input layer and k^{th} neuron of hidden layer. Similarly, w_j^3 is the weight connection between k^{th} neuron of hidden layer and single neuron of output layer and η is the Tan-sigmoid transfer function [24].

The objective function for minimization is verified through the root mean square error (RMSE) given in equation 15.

$$RMSE = \sqrt{\frac{1}{n}\sum_{1}^{n}\left(\frac{q_{actual}-q_{predicted}}{q_{actual}}\right)^2} \quad (15)$$

Where q_{actual} and $q_{predicted}$ are the actual output and predicted (network) output, respectively and n is the number of training data.

The main function of the CSO is to minimize the RMSE (given in equation 6) by tuning the weights and biases of FNN. The training was performed off line using a training set of 2600 samples. The connection weights were initially set at random values by the CSO, then modified iteratively until the stopping criteria is attained.

2.2 The CSO algorithm

The CSO technique is inspired by the intelligent foraging behaviour of chickens in a swarm. It has been shown in literature that the CSO algorithm has demonstrated superior performance in terms of both accuracy and robustness of the optimization results when compared to other popular optimization methods [25, 26]. This can be attributed to the multiple groups in the chicken swarm that are governed by several distinct laws [25]. Thus, the CSO can be viewed as a multi-swarm algorithm; hence the algorithms can more effectively explore the search space than single swarm algorithms. In addition, the CSO although operates with groups in a swarm, the algorithm still maintains a team [25]. Hence it can effectively strike a balance between exploration and exploitation of the search space.

The CSO algorithm is formulated by defining the positions of each individual chicken in the swarm. If *RN, HN, CN* and *MN* represent the number of roosters, hens, chicks and mother hens respectively, then, all *N* virtual chickens are defined by their positions $x_{i,j}^{t}$ $(i \in [1,2,3,\dots,N], j \in [1,2,3,\dots,D])$ at time *t*. where *N* is the total population of chickens in the swarm and *D* is the dimension or boundary within which the chickens search for food.

The roosters with better fitness value can search for food in a wider range than those with the worst fitness values. This is defined by the position equations 16 and 17 [25, 26].

$$x_{i,j}^{t+1} = x_{i,j}^{t} * \left(1 + Randn(0,\sigma^2)\right) \quad (16)$$

$$\sigma^2 = \begin{cases} 1, & if \quad f_i \le f_k \\ exp\left(\frac{f_k - f_i}{|f_i|+\varepsilon}\right), & otherwise \end{cases} \quad (17)$$

Where $k \in [1,N], k \neq i$, $Randn(0,\sigma^2)$ is a Gaussian distribution with standard deviation σ^2, ε is the smallest constant used to avoid zero division, k is the rooster's index and f is the fitness value.

For the hens, the dominant would have more advantage in competing for food than the passive ones. This can be formulated as shown in equation 18 - 20 [25]:

$$x_{i,j}^{t+1} = x_{i,j}^{t} + S1 * Rand[0,1] * \left(x_{r1,j}^{t} - x_{i,j}^{t}\right) + S2 * Rand[0,1] * \left(x_{r2,j}^{t} - x_{i,j}^{t}\right) \quad (18)$$

$$S1 = exp\left(\frac{f_i - f_{r1}}{abs(f_i)+\varepsilon}\right) \quad (19)$$

$$S2 = exp(f_{r2} - f_i) \quad (20)$$

Where $r1 \in [1,2,3,\dots,N]$ is the rooster's index in the i^{th} group, while $r2 \in [1,2,3,\dots,N]$ is the index of chicken (rooster or hen) randomly chosen from the swarm, but $r1 \neq r2$.

The chicks forage for food around their mother. This feature is formulated by equation 21 [25].

$$x_{i,j}^{t+1} = x_{i,j}^{t} + FL * \left(x_{m,j}^{t} - x_{i,j}^{t}\right) \quad (21)$$

Where $x_{m,j}^{t}$ is the position of the i^{th} chick's mother $(m \in [1,N])$. The parameter $FL(FL \in [0,2])$ is randomly chosen to determine the distance of the chick from its mother.

The six parameters: *RN, HN, CN, MN, G and FL* must be correctly specified in the CSO algorithm. As suggested in [25, 26], $RN = 0.2N, HN = 0.6N, CN = N - RN - HN, MN = 0.1N$ generally work well for most optimization problems. However, the selection of the appropriate value for *G* is problem specific. If *G* is very large, the convergence rate of the algorithm becomes slow while very small value may result in the algorithm converging to a local optimal solution. Generally, it is recommended that $G \in [2,20]$ and $FL \in [0.4,1]$ may give good results for most problems [25].

3. Results and discussion

In this paper, a 100kW standalone PV system is used for test and validation of the proposed CSO-MPPT algorithm. Soltech 1STH-215-P PV panels of the specifications listed in Table 1 [27] are used with 10 series connected modules and 47 parallel strings to generate the required 100kWp power.

Table 1: Solar Panel specifications

Specification	Value
Maximum power (p_{max})	215Wp $\pm 5\%$
Open circuit voltage (v_{oc})	36.300
Short circuit current (i_{sc})	7.840
Maximum power voltage (v_{mpp})	29.000
Maximum power current (i_{mpp})	7.350
Temperature coefficient of i_{sc} (α)	0.102
Temperature coefficient of v_{oc} (β)	-0.361

Figure 5 shows the complete simulation diagram developed in the MATLAB/SIMULINK environment. The PV system delivers power to a variable DC load through the DC-DC boost converter. The CSO-MPPT is compared with the conventional P&O algorithm. The internal blocks of the proposed CSO-ANN MPPT outlined in Figure 5 are detailed in Figure 6.

3.1 Simulation results

The ANN model is first trained using measured irradiance and temperature data for Yola, Adamawa State, Nigeria. The data is the daily average temperature and solar radiation for one year as shown in Figure 7 (a) and (b) respectively. These set of data serve as the inputs to the ANN and the target data is the voltage at maximum power point which is obtained via simulation in MATLAB.

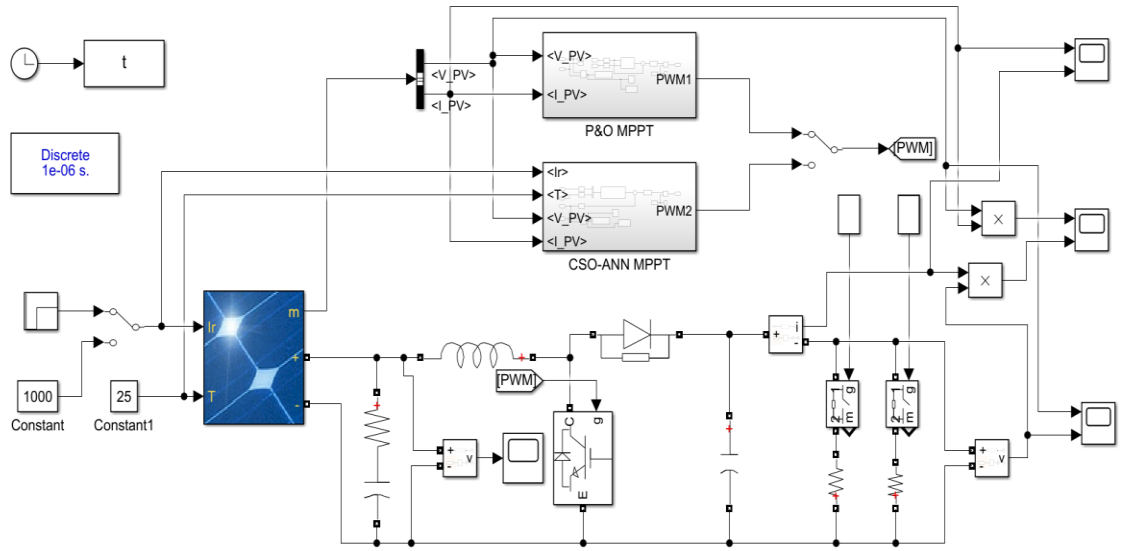

Figure 5: Diagram of the complete system

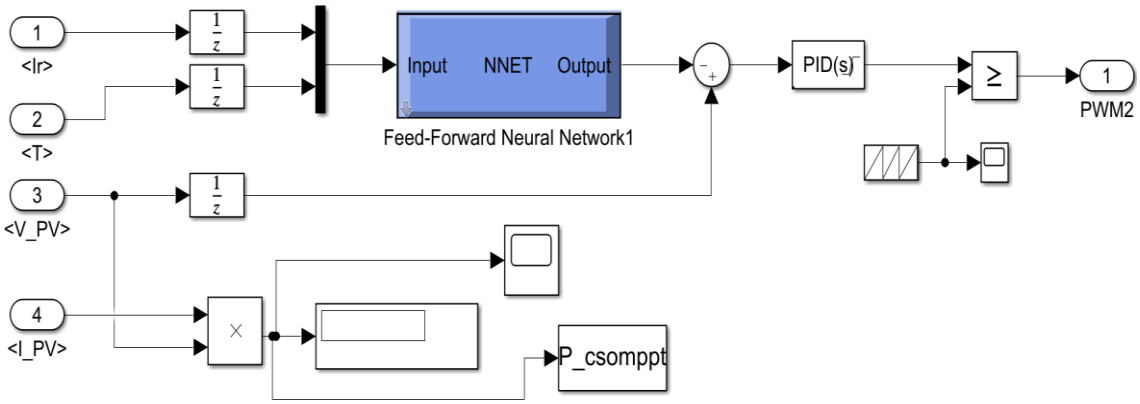

Figure 6: The CSO-Artificial Neural Network based MPPT

The CSO algorithm was used during the ANN training for obtaining optimum neurons weights and bias. This method has faster convergence rate when compared to the conventional back propagation method. Figure 8 shows the CSO convergence profile with the fitness function converging at just 53 iterations to a value of 0.073.

After the training, the simulations were conducted based on four different operating conditions in order to obtain the training data. These operating scenarios are listed as follows:

a. Case 1: Irradiance and temperature were kept constant at $1000W/m^2$ and 25^0C respectively. Also, load is kept constant.
b. Case 2: Irradiance and temperature were kept constant but load was increased by 20% at time 0.25s.
c. Case 3: Irradiance was varied while maintaining a constant load.
d. Case 4: Both irradiance and load were varied.

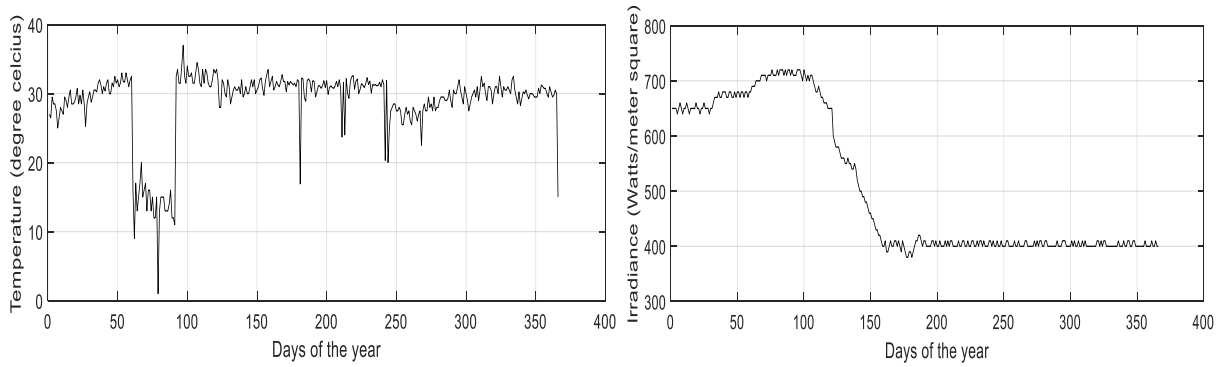

(a) (b)

Figure 7: Measured data for training ANN (a) Average daily temperature (b) Average daily irradiance

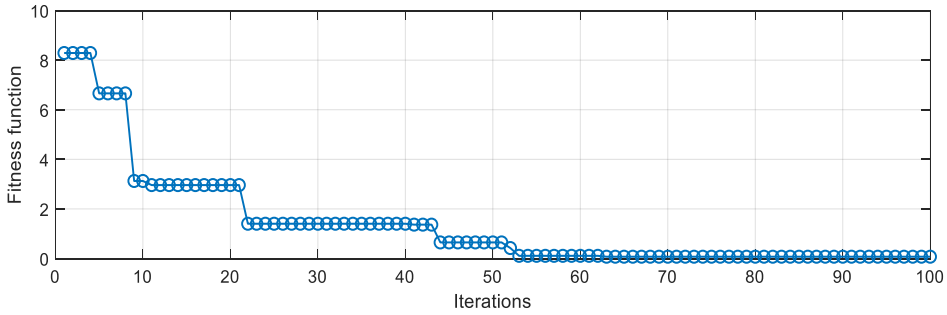

Figure 8: Convergence profile of the ANN using the CSO Algorithm

3.1.1 Case 1: Constant irradiance, temperature and load

Performance of the conventional P&O MPPT and the CSO-Tuned ANN MPPT controller are compared. Figs. 9 (a) and (b) show the PV power and load power for the CSO-ANN MPPT controller and P&O respectively. As can be observed, the proposed method results in smoother response with less ripples when compared to the conventional P&O MPPT. The percentage ripple factors for the CSO-Tuned ANN MPPT and the P&O MPPT were determined using equation 22. While both methods tracked the MPP fast, the P&O method shows greater output power fluctuations as can be clearly observed in in Figure 10 (b).

$$P_{ripple} = \frac{\sqrt{P_{peak}^2 - P_{rated}^2}}{P_{rated}} \times 100 \qquad (22)$$

Where P_{peak} is the peak-to-peak power

The calculated P_{ripple} factor based on Figure 10 (which presents zoomed-in sections of Figure 9) was 32.02% for the P&O method. In contrast, the proposed CSO-ANN MPPT method achieved a significantly lower ripple factor of 10.01%.

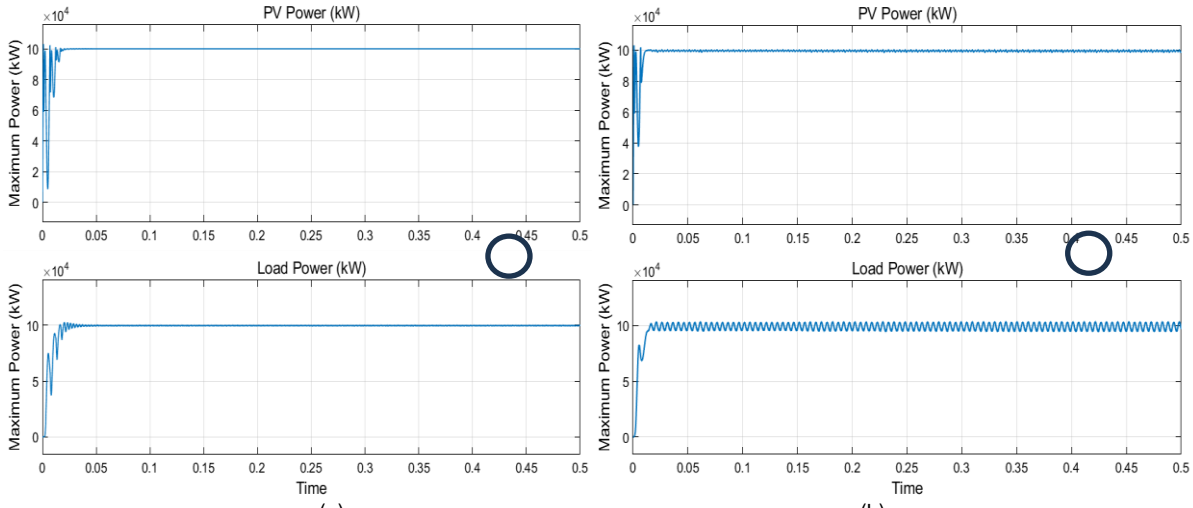

(a) (b)

Figure 9: Comparison of PV power and Output Power (a) CSO-ANN MPPT controller (b) P&O based MPPT controller

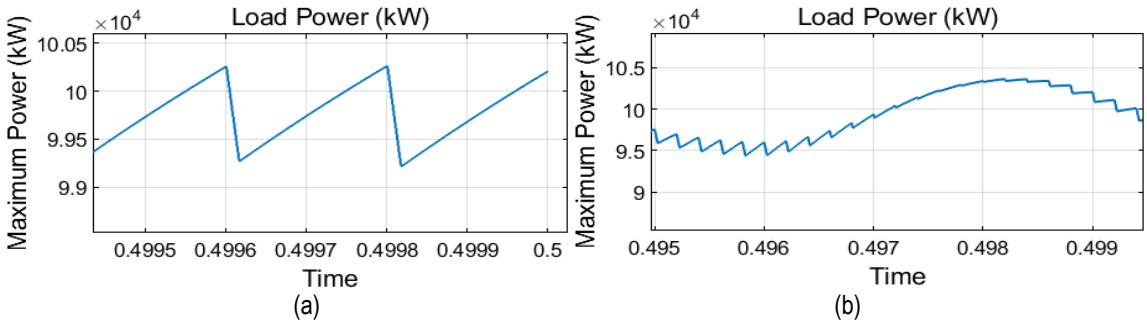

(a) (b)

Figure 10: Zoomed output power for ripple factor calculation (a) CSO-ANN MPPT controller (b) P&O based MPPT controller

In addition, the results for PV current and output current are also compared as shown in Figure 11 (a) and (b) respectively. Much higher ripples in the current can be observed when the P&O MPPT was deployed. However, in terms of tracking time, booth methods are fast, but for the P&O that comes as a trade-off for output power fluctuations.

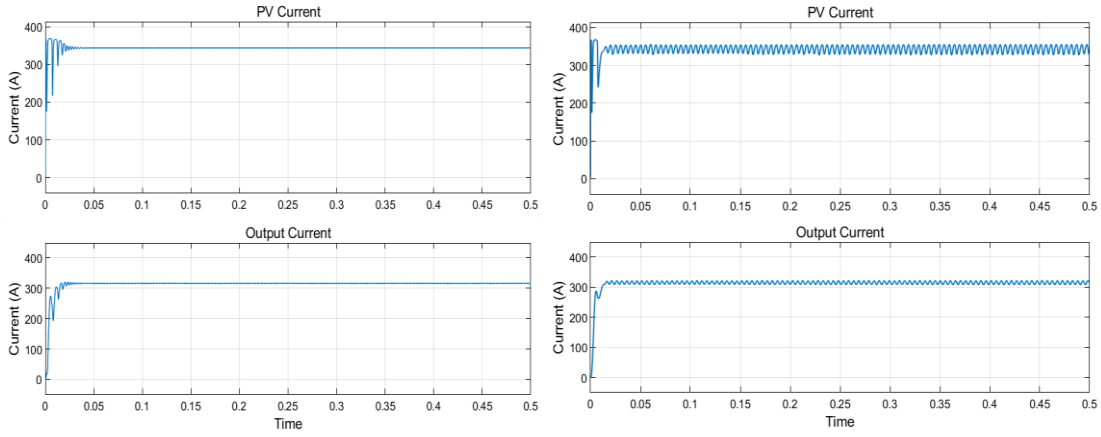

(a) (b)

Figure 11 Comparison of PV and output currents (a) CSO- ANN MPPT controller (b) P&O MPPT controller

3.1.2 Case 2: Constant irradiance and temperature with variable load

In this case, the load was increased by 20% at time 0.25s. The PV and load power as well as the voltage and currents of the PV and load were compared for both CSO-Tuned ANN MPPT controller and the conventional P&O MPPT controller. Based on Figure 12, the maximum power tracking remains the same for the two methods after the load was increased. However, prior to this, the P&O method shows significant oscillations in the output power, which is an inherent disadvantage of this method [28].

In terms of the voltages and currents; as the load is increased, reduction in voltage occurs, but this reduction is accompanied by an increase in current as can be seen in Figure 13. Hence the power slightly increased and remains constant at the maximum point as shown in Fig, 12 (c) and (d) for both methods.

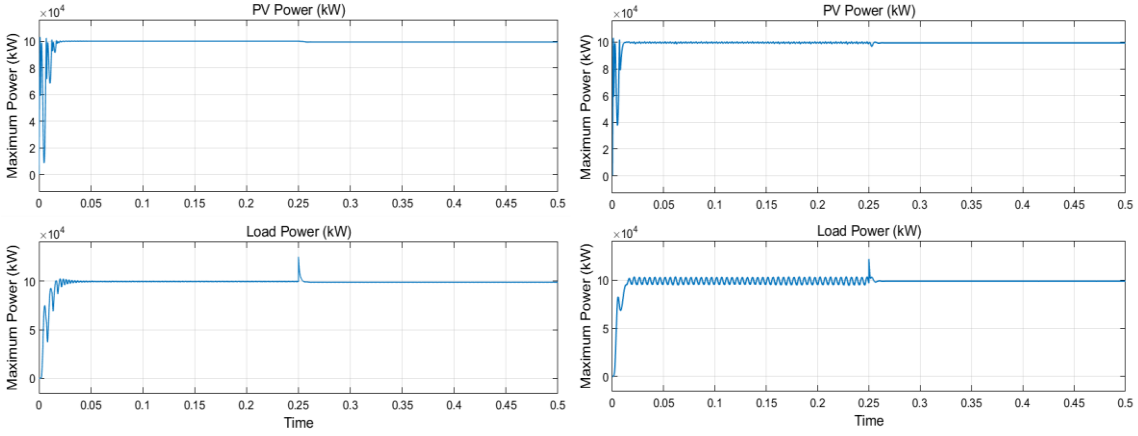

(a) (b)

Figure 12: Maximum power point tracking with change in load using (a) CSO- ANN MPPT controller (b) P&O MPPT controller

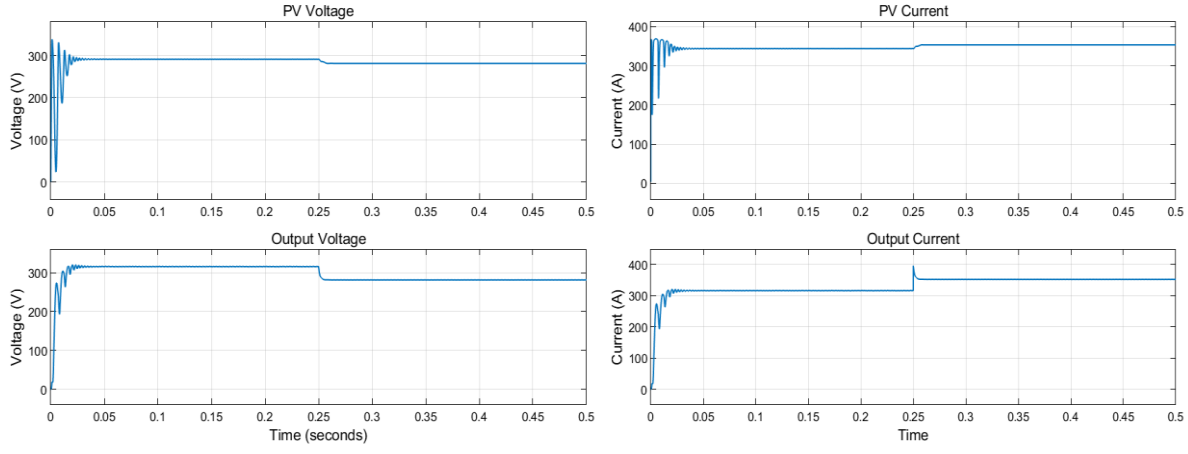

(a) (b)

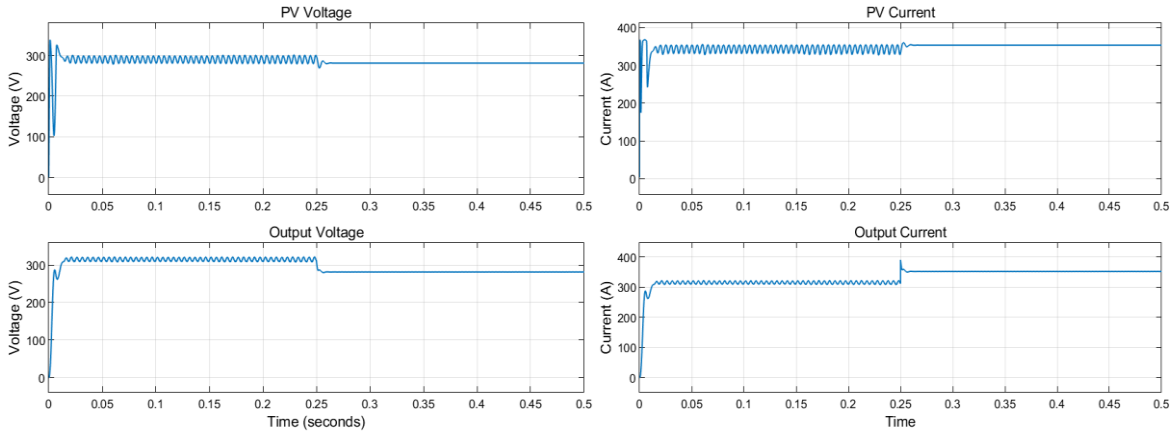

(c) (d)

Figure 13: PV and Output Voltages and Currents with change in load using (a&b) CSO- ANN MPPT controller (c&d) P&O MPPT controller

3.1.3 Case 3: Constant temperature and load with variable irradiance

Here, the irradiance was changed from $1000W/m^2$ to $500W/m^2$ at time $t = 0.2s$ and $800W/m^2$ at time $t = 0.3s$ and remains constant to the end of the simulation while load was kept constant.

The result using the proposed MPPT controller is shown in Figure 14(a). For comparison, the same case was used for the conventional P&O MPPT and the result is shown in Figure 14(b). As can be observed fast response and less ripples were recorded with the proposed MPPT controller.

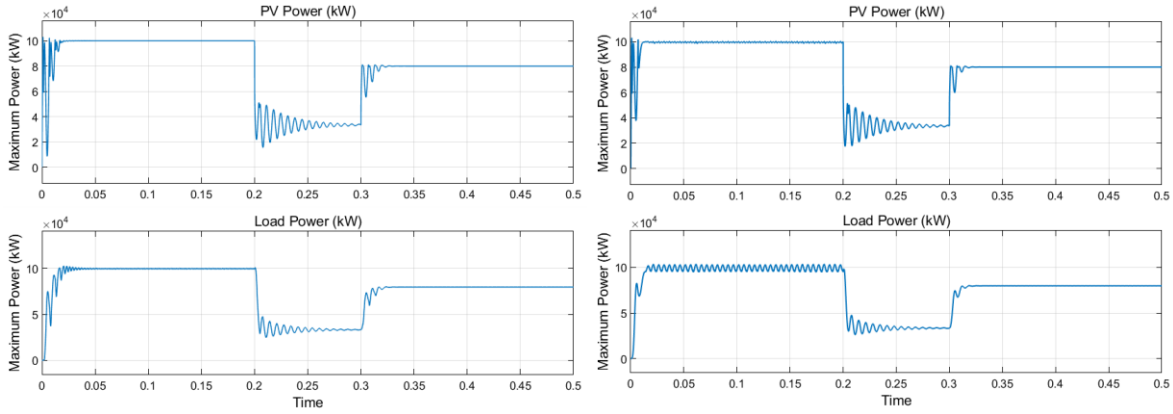

(a) (b)

Figure 14: Maximum power point tracking with change in Irradiance value using (a) CSO based ANN MPPT controller (b) P&O MPPT controller

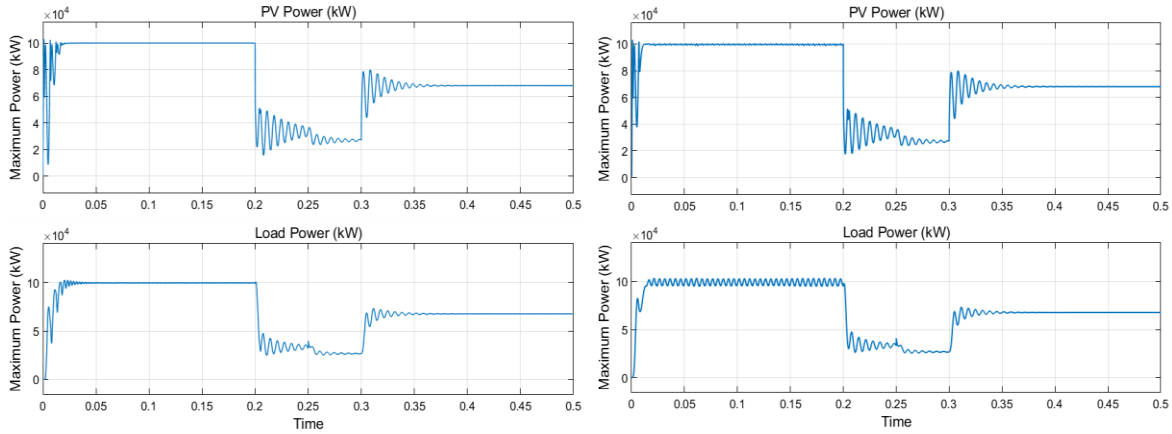

(a) (b)

Figure 14 Maximum power point tracking with change in Irradiance and load using (a) CSO based ANN MPPT controller (b) P&O MPPT controller

3.1.4 Case 4: Both irradiance and load were varied

For this case, both the irradiance and load were changed. The irradiance was varied from $1000W/m^2$ to $500W/m^2$ at time $t = 0.2s$ and $800W/m^2$ at time $t = 0.3s$ and remains constant to the end of the simulation. In addition, the load was increased by 20% at time $t = 0.25s$. Based on the results shown in Figure 15, it can be observed that the proposed CSO-ANN MPPT system was able to track the maximum power point in the presence of both changes in weather condition and load conditions. The system was fast and tracked the maximum power with little ripples when compared to the conventional P&O MPPT method.

4. Conclusion

This paper presented an optimized Artificial Neural Network (ANN)-based MPPT controller for photovoltaic (PV) systems, enhanced using the Chicken Swarm Optimization (CSO) algorithm. The proposed CSO-ANN model was trained under diverse operating conditions to ensure robust real-world performance. Simulation results demonstrated that the CSO-ANN MPPT outperformed the conventional Perturb and Observe (P&O) method, as it shows faster response, and smoothy adapt to variations in irradiance and load. In addition, the proposed CSO-ANN MPPT method was fast and has minimal ripples factor of 10.01% when compared to 32,02% achieved by the conventional P&O MPPT method.

The improved tracking accuracy and stability of the proposed system make it suitable for integration into grid-connected and standalone PV applications, especially in environments with rapidly changing weather conditions. The results obtained suggest strong potential for hardware implementation in next-generation smart solar inverters.

References

[1]. International Energy Agency, Renewables (2024). Analysis and forecast to 2028. Paris, France: IEA, 2024. [Online]. Available: https://www.iea.org/reports/renewables-2024.

[2]. Solar Power Europe, (2021), Global Market Outlook for Solar Power 2021–2025, Brussels, Belgium, 2021. [Online]. Available: https://www.solarpowereurope.org/insights/global-market-outlook

[3]. Sedaghati, F., Ali, N., Ali Badamchizadeh, M., Ghaemi, S., and Abedinpour Fallah, M. (2012). PV maximum power-point tracking by using artificial neural network. *Math. Problems Eng.* 2012 (1), 1–10. doi:10.1155/2012/506709.

[4]. Vidyanandan, K. V., (2017). An overview of factors affecting the performance of solar pv systems, energy scan, *A House Journal of Corporate Planning*, 27, 2 – 8.

[5]. Belghith, O. B., Sbita, L. and Bettaher, F., (2016). MPPT design using PSO technique for photovoltaic system control comparing to fuzzy logic and P&O controllers, *Energy and Power Engineering*, 8, 349-366. http://dx.doi.org/10.4236/epe.2016.811031.

[6]. Haitham, A., Mariusz, M. and Kamal, A., (2014). Power electronics for renewable energy systems, transportation and industrial applications, IEEE Press and John Wiley & Sons Ltd (2014), 160-184.

[7]. Elbarbary, Z. M. S. and Alranini, M. A., (2021). Review of maximum power point tracking algorithms of PV system, *Frontiers in Engineering and Built Environment*, 1(1), 68-80.

[8]. Satyajit, M., Bidyadhar, S. and Pravat, R., (2015). A new MPPT design using grey wolf optimization technique for photovoltaic system under partial shading conditions. *IEEE Transactions on Sustainable Energy*. 7. 1-8. http://dx.doi.org/10.1109/TSTE.2015.2482120.

[9]. Debnath, D., Soren, N., Pandey, A. D. and Barbhuiya, N. H., (2020). Improved grey wolf assists MPPT approach for solar photovoltaic system under partially shaded and gradually atmospheric changing condition. *International Energy Journal* 20(2020), 87 – 100.

[10]. Shixun, M., Qintao, Y., Kunping, J., Xiaofeng, M. and Gengyu, S., (2022). An improved MPPT method for photovoltaic systems based on mayfly optimization algorithm, *Energy Reports*, 8, 141-150. 10.1016/j.egyr.2022.02.160.

[11]. Bollipo, R. B., Mikkili, S. and Bonthagorla, P. K., (2021). Hybrid, optimal, intelligent and classical PV MPPT techniques: A review, *CSEE Journal of Power and Energy Systems*, 7(1), 9-33.

[12]. Mohapatra, A., Nayak, B., Das, P. and Mohanty, K. B., (2017). A review on MPPT techniques of PV system under partial shading condition, *Renewable and Sustainable Energy Reviews*, 80, 854-867.

[13]. Ebrahim, M. A., Osama, A., Kotb, K. M. and Bendary, F., (2019). Whale inspired algorithm based MPPT controllers for grid-connected solar photovoltaic system, *Energy Procedia* 162(2019), 77 – 86.

[14]. Villegas-Mier, C.G., Rodriguez-Resendiz, J., Álvarez-Alvarado, J.M., Rodriguez-Resendiz, H., Herrera-Navarro, A.M. and Rodríguez-Abreo, O., (2021). Artificial Neural Networks in MPPT Algorithms for Optimization of Photovoltaic Power Systems: A Review. *Micromachines*, 12, 1260. https://doi.org/10.3390/mi12101260.

[15]. Messalti, S., Harrag A. G. and Loukriz, A. E., (2015). A new neural networks MPPT controller for PV systems, *IREC2015 The Sixth International Renewable Energy Congress*, 2015, 1-6.

[16]. Al-Majidi, S. D., Abbod, M. F. and Al-Raweshidy, H. S., (2020). A particle swarm optimisation-trained feedforward neural network for predicting the maximum power point of a photovoltaic array, *Engineering Applications of Artificial Intelligence*, 92(2020), 0952-1976, https://www.sciencedirect.com/science/article/pii/S0952197620301238.

[17]. Li, H., Yang, D., Su, W., Lü J. and Yu, X., (2019). An overall distribution particle swarm optimization MPPT algorithm for photovoltaic system under

partial shading. *IEEE Transactions on Industrial Electronics, 66(1),* 65–75. http://dx.doi.org/10.1109/TIE.2018.2829668.

[18]. Liu J., Li J., Wu J. and Zhou W. (2017). Global MPPT algorithm with coordinated control of PSO and INC for rooftop PV array. The Journal of Engineering, 2017(13), 778–82. http://dx.doi.org/10.1049/joe.2017.0437.

[19]. Shixun, M., Qintao, Y., Kunping, J., Xiaofeng, M. and Gengyu, S. (2022). *An improved MPPT method for photovoltaic systems based on mayfly optimization algorithm*, The 2nd International Conference on Power Engineering (ICPE 2021), Nanning, Guangxi, China, Energy Reports, 8, 141–150.

[20]. Kaya, E., Ba¸stemur Kaya, C., Bende¸S. E., Atasever, S., Öztürk, B. and Yazlık, B., (2023). Training of Feed-Forward Neural Networks by Using Optimization Algorithms Based on Swarm-Intelligent for Maximum Power Point Tracking. *Biomimetics 2023, 8,* 402-406 https://doi.org/10.3390/biomimetics8050402.

[21]. Rekioua, D. and Matagne, E., (2012). Optimisation of Photovoltaic Power Systems, Modelization, Simulation and Control, Springer. http://dx.doi.org/10.1007/978-1-4471-2403-

[22]. Hussein A. Hussein A., Ali J., Mahdi B., Thamir M. and Abdul-Wahhab C., (2021). Design of a Boost Converter with MPPT Algorithm for a PV Generator Under Extreme Operating Conditions, *Engineering and Technology Journal 39 (10) (2021),* 1473-1480.

[23]. Razman, A. and Chee, W. T., (2018). Design of boost converter based on maximum power point resistance for photovoltaic applications, *Solar Energy, 160,* 322-335.

[24]. Pandey A., Panwar V. S., Hasan E. and Parhi D. R., (2020). V-REP-based navigation of automated wheeled robot between obstacles using PSO-tuned feedforward neural network, *Journal of Computational Design and Engineering,* 7(4), 427–434.

[25]. Meng, X., Liu, L. and Gao X. (2014). A new bio-inspired algorithm: chicken swarm optimization, in Advances in Swarm Intelligence, vol. 8794 of Lecture Notes in Computer Science, 86–94, Springer, 2014. https://www.springerprofessional.de/en/a-new-bio-inspired-algorithm-chicken-swarm-optimization/2293802.

[26]. Binhe, C., Li, C., Changzu, C., Yaodan, C. Yinggao, Y., (2024). A comprehensive survey on the chicken swarm optimization algorithm and its applications: state-of-the-art and research challenges, *Artificial Intelligence Review (2024),* 57-170. https://doi.org/10.1007/s10462-024-10786-3.

[27]. The MathWorks Inc. (2018). MATLAB version: (R2018b), Natick, Massachusetts: The MathWorks Inc. https://www.mathworks.com

[28]. Jubaer, A. and Zainal, S., (2015). An improved perturbs and observe (P&O) maximum power point tracking (MPPT) algorithm for higher efficiency, *Applied Energy*, 150, 97-108.